

Impact of inhomogeneous CMB heating of gas on the HI 21-cm signal during dark ages

Sioree Ansar,^{1,*} Kanan K. Datta,^{1,†} and Dhruba Dutta Chowdhury²

¹*Department of Physics, Presidency University, 86/1 College Street, Kolkata-700073, India*

²*Department of Astronomy, Yale University, New Haven, CT 06511*

(Dated: December 15, 2024)

Observations of redshifted HI 21-cm signal appear to be the most promising probe of the cosmic dark ages. The signal carries information about the thermal state along with density distribution of the intergalactic medium. The Cosmic Microwave Background Radiation (CMBR), through its interaction with charged particles, plays a major role in determining the kinetic and spin temperature of neutral hydrogen (HI) gas in the IGM during dark ages. Spatially fluctuating ionization fraction, which is caused by inhomogeneous recombinations, causes heat transfer from the CMBR to the IGM gas inhomogeneous. We revisit impact of this inhomogeneous heat transfer on spatial fluctuations in the observed HI 21-cm signal over a large redshift range during dark ages. Our study shows that the effect negatively impacts fluctuations in the HI spin temperature and results in enhanced HI 21-cm power spectrum. We find that the effect is particularly important during the transition of the gas kinetic temperature being coupled to the CMBR to fully decoupled from it i.e, in the redshift range $30 \lesssim z \lesssim 300$. It is found that, on the average the HI power spectrum $P_{T_b}(k, z)$ is enhanced by $\sim 4\%$, $\sim 10\%$, $\sim 20\%$ and $\sim 30\%$ at redshifts 60, 90, 140 and 200 respectively at $k = 0.1 \text{ Mpc}^{-1}$. The effect becomes even more significant at lower values of k_{\parallel}/k^2 due to reduced dominance of the peculiar velocity. It is observed that the power spectrum is enhanced by $\sim 49\%$ and $\sim 93\%$ at redshifts 140 and 200 respectively at $k = 0.1 \text{ Mpc}^{-1}$ for $k_{\parallel}/k^2 = 0$. This enhancement has a weak k -mode dependence.

PACS numbers: Valid PACS appear here

Introduction. The universe started becoming neutral during the cosmic recombination epoch. Subsequently, it passed through a long dark episode, known as the cosmic dark ages, when there was no source of visible light. Although an important event, this epoch could not be explored yet due to lack of observations. Observations using redshifted 21-cm signal from neutral hydrogen (HI) seem to be the only viable probe that has the potential to test and verify our current understanding of the dark ages by allowing the cosmological investigation of large scale matter density distribution and thermal history during the epoch[1, 2]. This can further be used to address some of the key cosmological questions regarding formation of first gravitationally bound objects[3], origin and formation of seed black holes[4], primordial non-gaussianity[5], dark matter decay and annihilation[6, 7], effect of primordial magnetic fields[8], variations in the fine structure constant[9] etc.

In the well established standard cosmological scenario, the evolution of the background universe and relevant physical processes that determine the strength of the HI 21-cm signal during dark ages are known with a high degree of accuracy. Further, the signal is not complicated by astrophysical processes unlike that during cosmic dawn and reionization epochs. This makes it possible to calculate the observable quantities i.e, the mean differential brightness temperature of HI 21-cm signal and its spatial fluctuations, which can be well approximated as linear up to very small scales, with a high level of precision.

A significant amount of work has already been done in order to understand both the globally averaged HI 21-cm signal and its spatial fluctuations during dark ages. Roles of underlying physical processes such as the recombination[10], coupling of the gas kinetic temperature with the background CMBR temperature, collisions between HI and other species[11], radiative coupling of the HI spin temperature with the background CMBR temperature that ultimately determine the redshift evolution of the HI differential brightness temperature and its fluctuations have been studied extensively (see[12] for a review).

This article focuses on the spatial fluctuations in the HI 21-cm differential brightness temperature. In particular, we highlight the role of inhomogeneous heat transfer from the CMBR to the IGM as an important contributor to the fluctuations. The fluctuations in ionization fraction make the heating of gas inhomogeneous. This contributes to the fluctuations in the gas kinetic temperature and, consequently, in the spin temperature. The effect has been included earlier [13, 15]. However, the focus was only at redshift ~ 50 where the effect was found to be negligible on the large scale HI 21-cm power spectrum. Here, we investigate and quantify, in detail, the impact of the effect on the HI 21-cm power spectrum over a large redshift range $30 \lesssim z \lesssim 300$. We adopt a simple analytical approach which clearly explains roles of various physical processes leading to the effect. We use cosmological parameters $(\Omega_{m0}, \Omega_{\Lambda0}, \Omega_{b0}h^2, h) = (0.3, 0.7, 0.02, 0.7)$, consistent with recent Planck measurements.

Basic 21-cm signal and evolution of mean quantities. The differential brightness temperature of HI 21-cm spin flip transition with respect to the CMBR temperature at redshift z can be written as[16]

$$T_b \approx \bar{T}(1 + \delta_b) \left(\frac{T_s - T_\gamma}{T_s} \right) \left(\frac{H(z)}{1 + z} \frac{1}{dv_{\parallel}/dr_{\parallel}} \right), \quad (1)$$

where $\bar{T} = 27 \text{ mK} x_{\text{HI}} \left(\frac{\Omega_{b0} h^2}{0.023} \right) \left(\frac{0.15}{\Omega_{m0} h^2} \frac{1+z}{10} \right)^{0.5}$. x_{HI} , δ_b and T_γ are the hydrogen neutral fraction, fractional over density in baryons and background CMBR brightness temperature respectively. The term $dv_{\parallel}/dr_{\parallel}$ is the gradient of proper velocity of HI gas along the line of sight. The spin temperature T_s is defined by the relation $\frac{n_1}{n_0} = \frac{g_1}{g_0} e^{-T_s/T_s}$, where n_1 and n_0 are the number densities of ground state HI in triplet and singlet states respectively, g_1 and g_0 are the respective degeneracies with $\frac{g_1}{g_0} = 3$. $T_* = \frac{h_p \nu_{21\text{cm}}}{k_B} = 0.068 \text{ K}$. During the dark ages T_s is mainly governed by two processes, 1. collisional coupling with the gas kinetic temperature T_g , and 2. radiative coupling with background CMBR. Therefore, the spin temperature during this epoch can be written as[17]

$$T_s^{-1} = \left(\frac{x_c T_g^{-1} + T_\gamma^{-1}}{1 + x_c} \right), \quad (2)$$

where $x_c = T_* C_{10} / A_{10} T_\gamma$ is the collisional coupling coefficient. A_{10} is the Einstein coefficient for spontaneous emission. $C_{10} = K_{10}^{\text{HH}} n_{\text{HI}}$ is the collisional de-excitation rate of HI from triplet to singlet state due to HI-HI collisions. n_{HI} is the number density of neutral hydrogen atom. We do not consider the HI-electron and HI-proton collisions as they are expected to play negligible roles in the redshift range of our interest. We use the fitting formula $K_{10}^{\text{HH}} = 3.1 \times 10^{-17} T_g^{0.357} e^{-\frac{32}{T_g}} \text{ m}^3 \text{s}^{-1}$ given in [12]. The redshift evolution of the gas kinetic temperature can be described by[9]

$$\frac{\partial T_g}{\partial z} = \frac{2T_g}{1+z} - \frac{32\sigma_T T_o^4 \sigma_{\text{SB}}}{3m_e c^2 H_o \sqrt{\Omega_{m0}}} (T_\gamma - T_g) (1+z)^{3/2} \frac{x}{1+x}, \quad (3)$$

where σ_T , σ_{SB} and $x = n_e/n_{\text{H}}$ are the Thomson scattering cross-section, Stefan Boltzmann constant and fractional ionization respectively. Here we assume $n_{\text{H}} = n_{\text{HI}} + n_{\text{HII}}$ and $n_{\text{HII}} = n_e$, assuming helium to be fully neutral. We see that the evolution of T_g is determined by two processes, 1. adiabatic cooling of HI gas due to universe's expansion (1st term, r.h.s) and 2. heat flow from the CMBR to gas through its interaction with free electrons (2nd term, r.h.s). Note that, T_g depends on the fractional ionization x which, at any redshift, is determined by the interplay between recombination and ionization processes. The ionization fraction x can be calculated at any redshift z before reionization using the

equation[10]

$$\frac{dx}{dz} = \frac{C}{H(z)(1+z)} \left[\alpha_e x^2 n_{\text{H}} - \beta_e (1-x) e^{-h_p \nu_\alpha / k_B T_g} \right], \quad (4)$$

where $C = \frac{1+K\Lambda(1-x)n_{\text{H}}}{1+K(\Lambda+\beta_e)(1-x)n_{\text{H}}}$ is the probability of a hydrogen atom at the first excited state jumping to the ground state without exciting an adjacent ground state atom, $\Lambda = 8.3 \text{ s}^{-1}$ is the two photon $2s \rightarrow 1s$ transition rate, $K = \frac{\lambda_\alpha^3}{8\pi H(z)}$ accounts for redshifting of Ly α photons due to universe's expansion, $h_p \nu_\alpha = 10.2 \text{ eV}$, α_e and β_e are the hydrogen recombination and photo-ionization coefficients respectively. Both quantities α_e and β_e depends on T_g and we use the functional forms given in [18, 19].

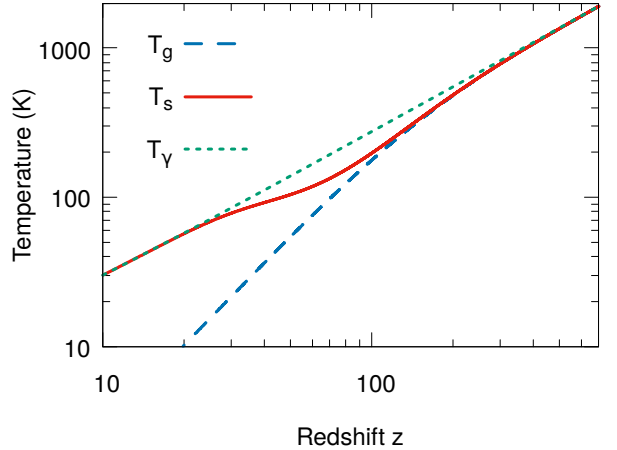


Figure 1. This plot shows the evolution of T_g , T_s and T_γ with redshift z .

Figure 1 shows the evolution of the CMBR (T_γ), spin (T_s) and gas kinetic temperature (T_g) with redshift. Note that the gas kinetic temperature (eq. 3) and ionization equations (eq. 4) are coupled and need to be solved together. We compare the solution for x obtained from eq. 4 with that from the RECFAST code [20] and find an excellent agreement. We also find that at lower redshifts $z \lesssim 750$, C becomes unity and the photo-ionization term becomes negligible compared to the recombination term in the ionization equation 4. As a consequence the ionization fraction x is essentially determined by the recombination and expansion rate of the universe at later redshifts. Heating of gas due to transfer of heat energy from the CMBR is very efficient at higher redshifts due to higher CMBR temperature and free electron (or gas) density. This keeps T_s coupled to T_γ at redshifts $z \gtrsim 300$. As universe expands adiabatically, both the free electron density and the CMBR temperature decrease, and the CMBR heating of gas becomes less effective in maintaining the gas temperature close to the CMBR temperature. Consequently, T_g starts to decouple from the CMBR and

falls below T_γ at redshifts $\lesssim 300$ and eventually scales as $(1+z)^2$ at redshifts $z \lesssim 30$. It means that the effects of CMBR heating of gas remains up to redshifts $z \sim 30$. The spin temperature T_s remains coupled to T_g up to redshifts $z \gtrsim 100$ through HI-HI, HI-electron, HI-proton collisions with the first one dominating over other two during the redshift range of our interest ($30 \lesssim z \lesssim 300$). As the HI gas density and T_g decrease collisions gradually become inefficient. Meanwhile the radiative coupling of T_s with T_γ takes over at later redshifts. Consequently, T_s starts to decouple from T_g at redshift $z \lesssim 100$ and tends towards the CMBR temperature.

Fluctuations in differential brightness temperature and impact of inhomogeneous CMBR heating. Radio interferometric experiments are sensitive to the spatial fluctuations in the 21-cm differential brightness temperature. The linear perturbation theory is adequate to quantify the fluctuations in the 21-cm signal at large scales during dark ages. It can be seen from eq. 1 that the fluctuations in the HI differential brightness temperature are a combination of fluctuations in baryon density, spin and CMBR temperature. The spin temperature fluctuations arise mainly due to the fluctuations in the gas kinetic temperature and collisional coupling x_c .

The fluctuation in baryon density is essentially same as that in hydrogen density $\delta_H(\mathbf{r}, z) = \frac{n_H(\mathbf{r}, z) - \bar{n}_H(z)}{\bar{n}_H(z)}$. Fluctuations in T_g , x and T_s are defined as $T_g(\mathbf{r}, z) = \bar{T}_g(z)[1 + \delta_g(\mathbf{r}, z)]$, $x(\mathbf{r}, z) = \bar{x}[1 + \delta_x(\mathbf{r}, z)]$ and $T_s(\mathbf{r}, z) = \bar{T}_s(z)[1 + \delta_s(\mathbf{r}, z)]$ respectively. The hydrogen density fluctuations, which trace the underlying dark matter (DM) density with a bias factor, essentially lead to fluctuations in all the above quantities. Thus we relate fluctuations in these quantities to the hydrogen density fluctuations as, $\delta_g = g(\mathbf{r}, z)\delta_H$, $\delta_x = m(\mathbf{r}, z)\delta_H$ and $\delta_s = s(\mathbf{r}, z)\delta_H$. Note that all δ_s , g , m , s are, in general, functions of spatial coordinates \mathbf{r} and redshift z but we do not show that explicitly hereafter. Using eqs. 3 and 4 we obtain equations for calculating redshift evolution parameters of linear fluctuations in gas kinetic temperature (g) and ionization fraction (m) as,

$$\frac{\partial g}{\partial z} = \left(\frac{2}{3} - g \right) \frac{1}{\delta_H} \frac{\partial \delta_H}{\partial z} + \frac{32\sigma_T T_o^4 \sigma_{SB}}{3m_e c^2 H_o \sqrt{\Omega_{m0}}} (1+z)^{3/2} \times \frac{\bar{x}}{1+\bar{x}} \left[\frac{T_\gamma}{\bar{T}_g} g - m \left(\frac{T_\gamma}{\bar{T}_g} - 1 \right) \right] \quad (5)$$

and,

$$\frac{\partial m}{\partial z} = -\frac{m}{\delta_H} \frac{\partial \delta_H}{\partial z} + \frac{\bar{C}}{H(z)(1+z)} \left[\bar{\alpha}_e \bar{n}_H \bar{x} \times \left(\frac{\delta_C + \delta_\alpha}{\delta_H} + 1 + m \right) - \bar{\beta}_e e^{-h_p \nu_\alpha / k_B \bar{T}_g} \times \left\{ \frac{m}{\bar{x}} + \frac{(1-\bar{x})}{\bar{x}} \left(\frac{\delta_C + \delta_\beta}{\delta_H} + g \frac{h_p \nu_\alpha}{k_B \bar{T}_g} \right) \right\} \right]. \quad (6)$$

δ_i is the first order perturbation term in i th quantity ($i = \alpha, \beta, C$), where $\delta_\alpha = \frac{\partial \alpha_e}{\partial T_g} \frac{\bar{T}_g}{\alpha_e(\bar{T}_g)} \delta_g$, $\delta_\beta = \frac{\partial \beta_e}{\partial T_g} \frac{\bar{T}_g}{\beta_e(\bar{T}_g)} \delta_g$ and $\delta_C = \frac{1}{\bar{C}} \left(\frac{\partial C}{\partial T_g} \bar{T}_g g + \frac{\partial C}{\partial x} \bar{x} m + \frac{\partial C}{\partial n_H} \bar{n}_H \right) \delta_H$. Note that eq. 5 is same as the eq. 25 in [15] and eq. 6 in [14] but represented differently. Eq. 6 is equivalent to the eq. 30 of [15] and eq. 3 of [14] if we neglect the photo-ionization term β_e and take $C = 1$ which are true for low redshifts. We ignore fluctuations in the CMBR temperature as it is found to be smaller compared to others in the redshift range of our interest. We note that the quantity δ_H traces the dark matter density distribution at large scales and lower redshifts. In these situations the quantity “ $\frac{1}{\delta_H} \frac{\partial \delta_H}{\partial z}$ ” reduces to $\frac{-1}{1+z}$. However, we do not make any such assumption and explicitly calculate the quantity “ $\frac{1}{\delta_H} \frac{\partial \delta_H}{\partial z}$ ” for different k -modes.

We use eq. 2 and find the redshift evolution parameter of linear fluctuations in the spin temperature as,

$$s = \frac{x_c}{1+x_c} \left[g \frac{\bar{T}_s}{\bar{T}_g} - \left(\frac{\bar{T}_s}{\bar{T}_g} - 1 \right) \left\{ 1 + g \frac{d(\ln K_{10}^{HH})}{d(\ln T_g)} \right\} \right]. \quad (7)$$

We note that, eqs. 5 and 6 are coupled i.e, the fluctuations in the fractional ionization and the kinetic temperature influence each other and eventually affect the fluctuations in spin temperature. This is due to the fact that higher amount of ionization fraction causes the CMBR heating of gas more efficient and thus makes gas hotter and vice versa.

The spatial fluctuations in the HI differential brightness temperature, defined as $T_b(\mathbf{r}, z) = \bar{T}_b(z) + \delta T_b(\mathbf{r}, z)$, is shown to be directly dependent on the fluctuations in hydrogen density δ_H , dark matter density δ_{DM} , and spin temperature as [1],

$$\delta T_b(\mathbf{r}, z) = \bar{T}(z) \left[\left(1 - \frac{T_\gamma}{\bar{T}_s} + \frac{T_\gamma}{\bar{T}_s} s \right) \delta_H + \mu^2 \left(1 - \frac{T_\gamma}{\bar{T}_s} \right) \delta_{DM} \right], \quad (8)$$

where $\mu = \cos \theta$ and θ is the angle between the line of sight and k -mode. The second term inside the third brackets arises due the peculiar velocity of HI gas. In the above equation we neglect the fluctuations in x_{HI} as including it shall result in addition of a term proportional to $\bar{x}m(z) \left(1 - \frac{T_\gamma}{\bar{T}_s} \right)$ which is $O(10^{-5})$ in the redshift range of interest. The HI 21-cm Power spectrum $P_{T_b}(k, z)$ can

be directly linked to the dark matter matter Power spectrum $P(k, z)$ as follows,

$$P_{T_b}(k, z) = \bar{T}^2(z) \left[\left(\frac{T_\gamma}{T_s} - s \frac{T_\gamma}{T_s} - 1 \right) b(k, z) + \mu^2 \left(\frac{T_\gamma}{T_s} - 1 \right) \right]^2 P(k, z) \quad (9)$$

where $\delta_H = b(k, z)\delta_{DM}$. $b(k, z)$ significantly differs from unity at redshift range and scales of our interest [3, 13] and impacts our results. This quantity has been calculated using CLASS software [21, 22]. Apart from the mean quantities and the underlying DM power spectrum, the HI 21-cm power spectrum depends on fluctuations in the spin temperature through s which is related to fluctuations in the kinetic temperature and coupling coefficient (see eq. 7). This tells us that fluctuations in the kinetic temperature g , which is caused by inhomogeneous CMBR heating of gas, ultimately affect the HI 21-cm power spectrum. We discuss this in detail in the subsequent section.

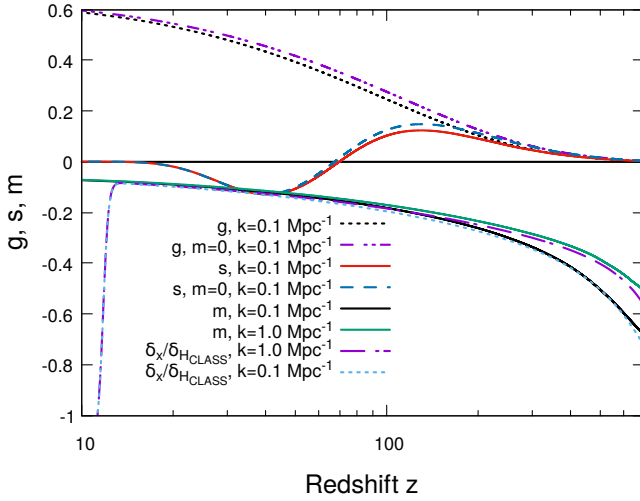


Figure 2. This plot shows the redshift evolution of $m(z)$, $g(z)$ & $s(z)$ in situations when the effect of inhomogeneous CMBR heating of gas is considered ($m(z) \neq 0$) and not considered ($m(z) = 0$). $m(z)$ has been shown for two k -modes. The quantity $\delta_x/\delta_{H\text{CLASS}}$ which is essentially same as $m(z)$ has been calculated using CLASS software.

Results. Figure 2 shows the redshift evolution of the kinetic (g), spin temperature (s) fluctuations at $k = 0.1 \text{ Mpc}^{-1}$ and ionization fraction fluctuations (m) at $k = 0.1 \text{ Mpc}^{-1}$ and $k = 1.0 \text{ Mpc}^{-1}$ respectively. These quantities are set to zero at very high redshift as they are highly coupled to the CMBR and thus expected to have negligible initial fluctuations. In order to solve equations 5 & 6 we first obtain δ_H as a function of redshift z at different k -modes from the CLASS software [21, 22] and then compute $\frac{1}{\delta_H(k, z)} \frac{\partial \delta_H(k, z)}{\partial z}$ which is essentially same as

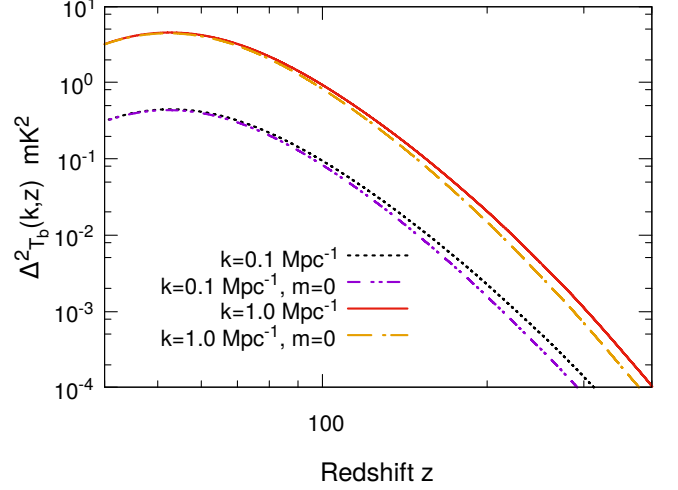


Figure 3. This plot shows redshift evolution of dimensionless HI 21-cm power spectrum $\Delta_{T_b}^2(k, z) = k^3 \times P_{T_b}(k, z)/2\pi^2$ for two k -modes for $m = 0$ (no inhomogeneous CMBR heating) and $m \neq 0$.

$\frac{1}{\delta_H(r, z)} \frac{\partial \delta_H(r, z)}{\partial z}$. Initially, at higher redshifts the photo-ionization plays a major role in determining the ionization fraction x as the CMBR temperature is higher and coupled to the gas temperature. However, the recombination process starts dominating at $z \lesssim 1200$ over the photo-ionization and, therefore, $m \rightarrow -1$. This means places with higher gas density have lower ionization fraction because the recombination rate, which is proportional to the gas density, is higher there. As the redshift further decreases, expansion of the universe plays a significant role in determining m and as a consequence $m \rightarrow 0$ at later redshifts. Figure 2 also compares evolution of m obtained directly from CLASS [21] software (by taking the ratio of fluctuations in ionization fraction δ_x and baryon density δ_H) with the same calculated using eq. 6 for two k -modes 0.1 and 1.0 Mpc^{-1} and they agree with each other quite well. Reionization due to stellar sources starts at redshift $z \sim 15$ in the model considered in CLASS which leads to the deviation in m observed at redshift $z \lesssim 15$.

Next we find that g , the redshift evolution parameter of linear fluctuations in the gas kinetic temperature, is considerably impacted by the inclusion of fluctuations in the ionization fraction, particularly at redshifts $z \lesssim 300$. In general, g is effectively zero at redshifts $z \gtrsim 300$ when T_g is highly coupled to T_γ . It starts to increase from redshift $z \sim 300$ and tends to a value $2/3$ as redshift decreases - a condition for a gas expanding pure adiabatically. However, as we discuss above, ionization fraction is inhomogeneously distributed. As a result the CMBR heating of gas, which depends on ionization fraction x (see eq. 4), becomes inhomogeneous too. Places with higher gas density, which have lower ionization fraction,

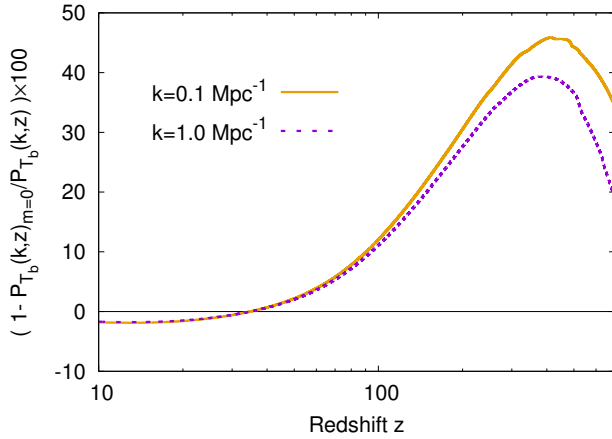


Figure 4. This plot shows redshift evolution of the percentage change in the HI 21-cm power spectrum due to inhomogeneous CMBR heating for two k -modes and $\mu^2 = 0.5$.

are less efficient in transferring heat from the CMBR to gas. Consequently, higher density places, which normally have higher gas kinetic temperatures ($g > 0$), will be negatively impacted by the inclusion of the inhomogeneous CMBR heating caused by in-homogeneous ionization fraction. This fact is manifested in eq. 5 which contains “ $-m(T_\gamma/T_g - 1)$ ” inside the second term in the rhs. For this reason g gets lowered when the effects of inhomogeneous CMBR heating of gas is considered. Obviously, the effect is negligible at higher redshifts as T_g and T_γ are coupled. It becomes important when T_g starts to decouple from the CMBR and g grows separately at redshift $z \sim 300$. It continues to be important up to redshifts at which the CMBR heating of gas still plays a significant role in determining T_g . In other words, inhomogeneous CMBR heating of gas is an important contributor to the gas kinetic temperature fluctuations during the transition period of T_g from being fully coupled to the CMBR to fully de-coupled from it. The other effect that could, in principle, affect the evolution of g , m and all subsequent results is the spatial fluctuations in the CMBR density. We consider this effect and find to have negligible impact on both quantities in the redshift range of our interest.

The redshift evolution parameter of linear fluctuations in the spin temperature s closely follows g at redshifts $z \gtrsim 200$ and, therefore, gets suppressed when the effect of in-homogeneous CMBR heating of gas is included. This is a consequence of the fact that the spin temperature T_s including its fluctuations remains coupled with T_g through collisional coupling at high redshifts. This can also be understood from eq. 7. Thereafter, s starts to unfollow g as collisions, which depend on T_g and HI density, become less efficient. Later s becomes negative and eventually tends to zero at lower redshifts. We note that s gets suppressed in redshifts range $30 \lesssim z \lesssim 200$. Although the generic nature of redshift evolution of m , g

and s remains same for different k -modes, we find them to mildly increase with k -modes in the redshift range of our interest.

We finally investigate the effect of inhomogeneous CMBR heating of gas on the power spectrum of HI 21-cm brightness temperature fluctuations. From eq. 9 we see that s is directly linked to the power spectrum in a way that a suppression of the spin temperature fluctuations leads to an increment in the power spectrum. Fig. 3 plots the dimensionless HI 21-cm power spectrum $\Delta_{Tb}^2(k, z) = k^3 \times P_{Tb}(k, z)/2\pi^2$ for two k -modes for the case when the inhomogeneous CMB heating is considered in the evaluation of s and compares with the case when the effect is not considered i.e, $m = 0$. We assume μ^2 to be ~ 0.5 . We obtain a considerable enhancement in the HI brightness temperature power spectrum $P_{Tb}(k, z)$ for the first case. At the redshift $z \sim 50$, the enhancement in the HI Power spectrum is $\sim 2\%$. This is in good agreement with the results reported in [13, 14]¹. Further, we find that the HI Power spectrum $P_{Tb}(k, z)$ is enhanced by $\sim 4\%$, $\sim 10\%$, $\sim 20\%$ and $\sim 30\%$ at redshifts 60, 90, 140 and 200 respectively at $k = 0.1 \text{ Mpc}^{-1}$ when the inhomogeneous CMB heating of gas is considered (see Fig. 4). We also notice that this enhancement has a weak dependence on k -modes. Although the percentage change is even greater at higher redshifts the absolute change in the power spectrum i.e, the quantity $(P_{Tb} - P_{Tb, m=0})$ becomes insignificant as T_s becomes coupled to T_γ . The enhancement in the power spectrum can be explained using eq. 9 which shows power spectrum’s dependence on s . As we discuss above s gets suppressed when the effect of inhomogeneous CMBR heating of gas is included.

Although, the above paragraph discusses results for $\mu^2 = 0.5$, the effect on the power spectrum $P_{Tb}(k, z)$ would be different for different values of μ^2 (see in eq. 9) which varies from 0 to 1. For higher values of μ^2 , contribution from the peculiar velocity effect, which is insensitive to the inhomogeneous heating, becomes higher. This reduces the overall effect of the inhomogeneous heating on the HI power spectrum $P_{Tb}(k, z)$. For $\mu^2 = 1$, we find that $P_{Tb}(k, z)$ is enhanced just by $\sim 1.7\%$, $\sim 2.7\%$, $\sim 6.4\%$, 11.5% and $\sim 16\%$ at redshifts around 50, 60, 90, 140 and 200 respectively at $k = 0.1 \text{ Mpc}^{-1}$. On the other hand, the changes are considerably higher at $\sim 3\%$, $\sim 5\%$, $\sim 17.5\%$, 49% and $\sim 93\%$ at redshifts around 50, 60, 90, 140 and 200 respectively at $k = 0.1 \text{ Mpc}^{-1}$ for $\mu^2 = 0$. However, we note that, the observed signal at modes corresponding to $\mu^2 \lesssim \frac{C^2}{C^2+1}$ will be highly dominated by contributions from strong foreground sources. Here C is a function of both the antenna primary field

¹ We note that, [13, 14] looked at the effects on the angular power spectrum C_l where as we focus on $P_{Tb}(k, z)$. These two different statistical quantities can be compared only for an ‘average’ value of μ^2 which is assumed to be 0.5.

of view and redshift z [23]. Thus, these modes may be avoided while extracting the HI 21-cm power spectrum from observed data. On the other hand, some small k_{\perp} modes are not available in radio interferometric observations due to lower baseline cut-off. This poses restrictions on using modes corresponding to $\mu^2 \sim 1$. Consequently, the intermediate modes centred around $\mu^2 \sim 0.5$ are likely to be more useful for HI 21-cm power spectrum measurements.

Summary and Discussion. Observations of redshifted 21-cm signal seem to be the only viable probe of cosmic dark ages. The kinetic temperature of the intergalactic neutral gas, which plays a major role in determining the HI 21-cm signal, is significantly affected during dark ages by the heat transfer from the CMBR to gas through its interaction with free electrons. The heat transfer from the CMBR to gas in the intergalactic medium depends on the ionization fraction which is inhomogeneously distributed in space mainly due to inhomogeneous recombination process. We investigate, in detail, the effect of inhomogeneous CMBR heating of gas on the HI 21-cm differential brightness temperature fluctuations over a large redshift range during dark ages. We follow a simple analytical formalism which clearly explains roles of relevant physical processes leading to the effect. We find that the inhomogeneous heating of gas causes an additional fluctuations in the kinetic temperature and, consequently, in spin temperature and ultimately in 21-cm signal. We also find that the effect has detectable signatures in the HI 21-cm power spectrum when the gas kinetic temperature T_g starts to decouple from the CMBR at redshift $z \sim 300$. The effect remains important down to redshift $z \sim 30$ up to which the CMBR heating of gas plays a significant role in determining T_g . In other words, the transition period of T_g being fully coupled to the CMBR to fully de-coupled from it remains important for the effect. Our results agree quite well with earlier studies which focus only on redshift ~ 50 and find a negligible effect on the HI power spectrum. However, we find that the HI power spectrum $P_{T_b}(k, z)$ is considerably enhanced by $\sim 4\%$, $\sim 10\%$, $\sim 20\%$ and $\sim 30\%$ at redshifts 60, 90, 140 and 200 respectively for $k = 0.1 \text{ Mpc}^{-1}$ and $\mu^2 = 0.5$. The effect becomes even higher for lower values of μ^2 due to the reduced influence of the peculiar velocity which is insensitive to the inhomogeneous heating. We also notice a mild change in our results at higher k -modes. At higher redshifts $z \gtrsim 300$ the effect makes negligible changes in observable quantities as the

spin temperature gets coupled to the CMBR temperature. The effect has its root in the underlying matter and gas density fluctuations and, therefore, is intrinsic to any calculation regarding HI 21-cm signal during dark ages. It has to be considered in every situation where the gas kinetic and spin temperature fluctuations play important roles.

Acknowledgements: KKD and DDC acknowledge financial support through a DST project SR/FTP/PS-119/2012. We thank Sk. Saiyad Ali for useful discussion and his help. We also thank CTS, IIT Kharagpur for a visit where a part of this work was done.

* sioreeansar@gmail.com

† kanan.physics@presiuniv.ac.in

- [1] Bharadwaj, S., & Ali, S. S. 2004, MNRAS, 352, 142
- [2] Loeb, A., & Zaldarriaga, M. 2004, Physical Review Letters, 92, 211301
- [3] Naoz, S., & Barkana, R. 2007, MNRAS, 377, 667
- [4] Tashiro, H., & Sugiyama, N. 2013, MNRAS, 435, 3001
- [5] Muñoz, J. B., Ali-Haïmoud, Y., & Kamionkowski, M. 2015, PRD, 92, 083508
- [6] Natarajan, A., & Schwarz, D. J. 2009, Phys. Rev. D, 80, 043529
- [7] Furlanetto, S. R., Oh, S. P., & Pierpaoli, E. 2006, Phys. Rev. D, 74, 103502
- [8] Schleicher, D. R. G., Banerjee, R., & Klessen, R. S. 2009, Astrophys. J., 692, 236
- [9] Khatri, R., & Wandelt, B. D. 2007, Physical Review Letters, 98, 111301
- [10] Peebles, P. J. E. 1968, Astrophys. J., 153, 1
- [11] Zygelman, B. 2005, Astrophys. J., 622, 1356
- [12] Pritchard, J. R., & Loeb, A. 2012, Reports on Progress in Physics, 75, 086901
- [13] Lewis, A., & Challinor, A. 2007, Phys. Rev. D, 76, 083005
- [14] Lewis, A. 2007, Phys. Rev. D, 76, 063001
- [15] Ali-Haïmoud, Y., Meerburg, P. D., & Yuan, S. 2014, Phys. Rev. D, 89, 083506
- [16] Furlanetto, S. R., Oh, S. P., & Briggs, F. H. 2006, Physics Reports, 433, 181
- [17] Field, G. B. 1958, Proceedings of the IRE, 46, 240
- [18] Seager, S., Sasselov, D. D., & Scott, D. 1999, ApJL, 523, L1
- [19] Seager, S., Sasselov, D. D., & Scott, D. 2000, ApJS, 128, 407
- [20] <http://www.astro.ubc.ca/people/scott/recfast.html>
- [21] <http://class-code.net/>
- [22] Lesgourgues, J. 2011, arXiv:1104.2932
- [23] Dillon J. S., et al., 2014, Phys. Rev. D, 89, 023002